



# Screening of process variables using Box–Behnken design in the fabrication of berberine hydrochloride-loaded transethosomes for enhanced transdermal delivery

Koushlesh Kumar Mishra<sup>1\*</sup>, Chanchal Deep Kaur<sup>2</sup>

<sup>1</sup>Shri Rawatpura Sarkar Institute of Pharmacy, Kumhari, Chhattisgarh, India

<sup>2</sup>Rungta College of Pharmaceutical Sciences and Research, Nandanvan, Raipur, Chhattisgarh, India

## Corresponding Author:

Mr. Koushlesh Kumar Mishra,  
Shri Rawatpura Sarkar  
Institute of Pharmacy,  
Kumhari, Chhattisgarh, India.  
E-mail: koushleshmishra@gmail.com

**Received:** June 08, 2021

**Accepted:** September 07, 2021

**Published:** March 23, 2022

## ABSTRACT

**Objective:** The objective of the present work was to develop, optimize, and characterize berberine hydrochloride (BBN-HCl)-loaded transethosomes (TEs) for enhanced transdermal delivery. In this study, screening of formulation and process variables was conducted using Box–Behnken design approach to observe significant and insignificant influence on the TEs. **Materials and Methods:** The TEs were developed by homogenization technique (hot method). The optimized BBN-HCl-loaded TEs were evaluated for its vesicle size (VS), polydispersity index (PDI), zeta potential (ZP), loading capacity, and entrapment efficiency. Characterization was done by powder X-ray diffraction (P-XRD), differential scanning calorimetric (DSC), and transmission electron microscopy. Further, *in vitro* drug release study, stability study, and confocal laser scanning microscopy (CLSM) study were also performed. **Results:** The BBN-HCl-loaded TEs are developed using soya lecithin as phospholipid, oleic acid as edge activator, and cholesterol as stabilizer. Developed TEs showed acceptable desired VS (185–435 nm), excellent colloidal dispersion characteristics (PDI – 0.141–0.321 and ZP – –17.34––24.35 mV), and high drug entrapment (67.05–85.21%). P-XRD and DSC results suggested that BBN-HCl encapsulated in amorphous state within TEs. *In vitro* drug release study shows prolonged release of BBN-HCl for 24 h and CLSM confirmed accumulation of TEs in deeper layers of the skin. Results of stability studies showed optimized TEs are more stable in refrigerated temperature (4°C) as compared to room temperature (25°C). **Conclusion:** The developed TEs successfully encapsulated berberine hydrochloride, yielding an increased permeation and deeper penetration. The results suggested that TEs could be better alternative to deliver drugs across the skin and potential carrier for efficient transdermal drug delivery.

**Keywords:** Transethosomes, Berberine hydrochloride, Box–Behnken design, Optimization, transdermal delivery

## INTRODUCTION

Drug delivery becomes apparent as a technique which consists of biopharmaceutics and pharmacokinetics. Nowadays, different types of drug delivery systems are available which enhance the efficacy of drugs in various treatments by controlled and sustained release. Novel drug delivery system improves mainly bioavailability, therapeutic index, and patient compliance.<sup>[1]</sup> For effective drug delivery, pre-formulation study is the one of the most important parameters for developing stable and bioavailable dosage form.

During the past few decades, researchers are working on delivering the active pharmaceutical ingredient through transdermal route but still the effective delivery of drug through the said route is challenging because of stratum corneum barrier problem.<sup>[2]</sup> Transethosomes (TEs) are newly effective lipid-based vesicular system which shows enhanced drug permeation through skin for transdermal drug delivery, extremely biocompatible and biodegradable, non-toxic, more stable, and patient compliance due to the avoidance of first-pass metabolism.<sup>[3]</sup> Transfersomes composed of phospholipid, surfactant, and water while ethosomes are consist of phospholipids, ethanol, and water. TEs are the

combination of transferosomes and ethosomes. It is composed of phospholipids, surfactant, ethanol, and water. The main disadvantages of transferosomes were difficulty of loading hydrophobic drugs into the vesicles without affecting their deformability and elastic properties.<sup>[4]</sup> While, in ethosomes, ethanol acts as a permeation enhancer and not contains edge activator but in TEs, these vesicles contain ethanol as well as edge activator or surfactants. Skin permeation of TEs was higher than the ethosomes and transferosomes. Drugs ranging from low molecular weight to high molecular weight can easily be entrapped by TEs. Due to their ultra-flexible biodegradable and biocompatible nature, it shows highly efficient entrapment ability.<sup>[5]</sup>

Berberine [ $C_{20}H_{18}NO_4^+$ ] is an important quaternary ammonium salt from the protoberberine group of benzyloquinoline alkaloid isolated from various plants such as *Berberis aristata* (tree turmeric), *Berberis vulgaris* (barberry), and *Hydrastis canadensis* (goldenseal).<sup>[6]</sup> Berberine possesses various promising pharmacological actions but due to its toxicity, its uses were limited. The studies show that it reduces atherosclerosis,<sup>[7]</sup> antimicrobial,<sup>[8]</sup> antiprotozoal,<sup>[9]</sup> antidiarrheal,<sup>[10]</sup> novel chemotherapeutic agent in the treatment of malignancy,<sup>[11]</sup> anticancer,<sup>[12]</sup> antidiabetic activity,<sup>[13]</sup> anti-hyperlipidemic activity,<sup>[14]</sup> antihypertensive effects,<sup>[15]</sup> antifungals,<sup>[16]</sup> and antibacterial.<sup>[17]</sup> Along with broad pharmacological actions, their insolubility or low aqueous solubility, toxicity, and stability limit their clinical applicability. Furthermore, berberine is also used in the field of formulation development. The study shows berberine nanoparticles shown promising activities against Gram-positive and Gram-negative bacteria with enhanced *in vitro* bioavailability.<sup>[18]</sup> Previously, it is also developed for niosomal drug delivery system as a non-ionic surfactant-based vesicles<sup>[19]</sup> and self-microemulsifying drug delivery system for oral bioavailability enhancement.<sup>[20]</sup>

All methods available for the preparation of TEs show various limitations, which are affecting directly or indirectly the quality of transethosome formulations. Nowadays, principles of quality by design adopt to ensure the quality of drug as it relates their safety and efficacy.<sup>[21]</sup> Nowadays, design of experiment methodology is most widely used for advancements study of novel drug delivery systems. It is a technique utilized for the assurance of connection between the different elements affected the procedure and the yields of the procedure. Experimental design can be applied to characterize the goal of examination, choose the nature of the reactions, number and nature of trial factors, and least number of trial runs.<sup>[22]</sup> Experimental design incorporates an underlying component screening and optimization by Box–Behnken design.<sup>[23]</sup>

The present study was focused on screening of process variables for the preparation of berberine hydrochloride (BBN-HCl)-loaded TEs for enhanced transdermal delivery. In this study, we emphasize herbal ethosomal technology. Box–Behnken design was utilized to screen the impact of different procedure and formulation factors. In this study, the chose plan and procedure factors were phospholipid concentration ( $X_1$ ), edge activator concentration ( $X_2$ ), ethanol concentration ( $X_3$ ), and sonication time ( $X_4$ ). The effects of the process and formulation factors on mean vesicle size (VS) ( $Y_1$ ), zeta potential (ZP) ( $Y_2$ ), polydispersity index ( $Y_3$ ),

and drug entrapment efficiency (EE) ( $Y_4$ ) were investigated. This work is the first step in the development of an optimized berberine hydrochloride nanovesicular preparation suitable for transdermal drug delivery.

## MATERIALS AND METHODS

### Materials

BBN-HCL was purchased from Indian Herbs Extractions Ltd., U.K, India, having 97% percentage purity. Ethanol, oleic acid, cholesterol, soya lecithin, and rhodamine-B were purchased from Sigma-Aldrich, New Delhi, India. All other reagents, chemicals, and solvents used for the study were of analytical grade.

### Instrumentation

The TEs was produced using hot homogenization method as reported earlier by Song *et al.* TEs prepared by some modifications in their previous reported method. A probe sonicator (Ultrasonic Homogenizer, Athena technologies, Mumbai, India) used for ultra-sonication. Homogenizer (Remi Elektrotechnik Ltd., Mumbai, India) is used for reducing into extremely small particles and distributing it uniformly throughout a fluid. RQ-122 used at 4000 rpm for 15 min. For release study, diffusion cell apparatus (Althea Technology, Thane, India) was used. The Delsa Nano C Particle analyzer (Beckman Coulter, DLS Zetasizer, California, USA) was used for the estimation of VS, ZP, and polydispersity index (PDI) value of transethosomal formulations. The UV–visible spectrophotometer (UV-1900i, Shimadzu, Japan) was used for determining the EE. Transmission electron microscopy (TEM) (TALOS-200 kv, S-FEG, FEI, USA) was used to study structure and surface morphology of TEs. Differential scanning calorimetric (DSC) (DSC 6000, Perkin Elmer, Waltham, USA) and PXRD (PANalytical Empyrean x-ray diffractometer in the Bragg-Brentano geometry using Cu-K $\alpha_1$ , Malvern Panalytical Ltd., UK) were used for characterization of formulations. Confocal laser scanning microscopy (CLSM) (Olympus-FV1200MPE, IX83 microscope, Tokyo, Japan) was used for drug permeation study of tissues.

### Methods

#### Preparation of BBN-HCl-loaded TEs

The BBN-HCl-loaded TEs were prepared by homogenization hot method as reported earlier by Song *et al.* (2012) with some modifications. First, BBN-HCl, soya lecithin, and oleic acid were dissolved in ethanol at 40°C followed by magnetic stirring at 700 rpm. Then, remaining aqueous phase was added slowly to ethanolic solution to obtain transethosomal dispersion. After getting smooth suspension, homogenization done using homogenizer (RQ-122, REMI Elektrotechnik Ltd., Vasai, India) at 6000 rpm for 20 min. Later on, obtained mixture was filtered through membrane filter and sonicate in ultrabath sonicator (Ultrasonic Homogenizer, Athena Technologies, Mumbai, India) to get desired size of TEs for optimization.

#### Experimental design (Box–Behnken design)

In this research work, we have adopted most proficient and powerful statistical model Box–Behnken screening design

(BBD) than the other designs to develop the BBN-HCl-loaded transethosomal formulations by conventional hot method. A 4-factor Box–Behnken design at two levels (high and low) was applied for the preliminary screening on VS, ZP, PDI, and EE. On the basis of previous experiments and literature reviews, low and high levels of the variables were selected. Box–Behnken experimental design of the statistical package Design-Expert® version 13 software (Stat-Ease Inc., Minneapolis, MN) was used to assess the effects of selected independent variables on the variables responses to optimize the BBN-HCl-loaded TEs formulation.<sup>[24]</sup>

The chosen independent variables were the concentration of lipid ( $X_1$ ), edge activator concentration ( $X_2$ ), concentration of ethanol ( $X_3$ ), and sonication time ( $X_4$ ). The observed response of the dependent variables was VS ( $Y_1$ ), ZP ( $Y_2$ ), PDI ( $Y_3$ ), and EE ( $Y_4$ ). A total of 24 experimental runs were planned by BBD under controlled circumstances [Table 1].

#### Characterization of BBN-HCl-loaded TEs

##### Determination of VS, PDI, and ZP of TEs

The VS and PDI of TEs were determined by dynamic light scattering (DLS) technique or photo correlation spectroscopy using a Delsa Nano C Particle analyzer (Beckman Coulter, Germany) at 25°C. For analysis, a minimum of 2 ml of the prepared suspension was transferred into 4–5 ml disposable plastic cuvette. It was placed in analysis device and subsequent analyzed for size analysis. All measurements were conducted at 90° scattering angle. The ZP was determined by Delsa Nano C Particle analyzer through measuring mobility and conductivity. The temperature and average electric field were applied at 25°C and 16 V/cm, respectively.<sup>[25]</sup> The mean value of three repeated measurements of every sample was reported as final result.

##### Drug loading and EE

Drug loading and encapsulation efficiency of BBN-HCl in TEs were estimated by the double beam UV–visible spectrophotometer (Shimadzu, Japan) at 429 nm wavelength. A 2 ml of BBN-HCl-loaded transethosomal suspension was centrifuged at 12,500 rpm for 15 min to separate the lipid and aqueous phase. The supernatant was discarded and berberine hydrochloride (BBN-HCl) was diluted with methanol. After this, drug content was determined by spectrophotometer.<sup>[26]</sup> Consequently, drug loading and EE calculation were done using the following equations:

$$DL (\%) = \frac{\text{Weight of BBN – HCl added} - \text{Weight of uncapsulated BBN – HCl}}{\text{Weight of lipid added}} \times 100 \quad \text{Eq (1)}$$

$$EE (\%) = \frac{\text{Weight of BBN – HCl added} - \text{Weight of uncapsulated BBN – HCl}}{\text{Weight of BBN – HCl added}} \times 100 \quad \text{Eq (2)}$$

##### Powder X-ray diffraction (P-XRD) study

The identification of amorphous and crystalline nature of sample is evaluated by X-ray powder diffraction (P-XRD). XRD patterns of the optimized BBN-HCl-loaded TEs, lyophilized empty TEs, pure BBN-HCl, cholesterol, and soya lecithin were collected with X-ray diffractometer (PANalytical Empyrean

**Table 1:** The independent and dependent variables with their levels and constraints in Box–Behnken design for the development of berberine hydrochloride-loaded TEs

Variables	Code	Low level	High level	Units
Independent variables				
Lipid concentration	$X_1$	1	3	% w/v
Edge activator conc.	$X_2$	20	80	mg
Ethanol concentration	$X_3$	20	40	% v/v
Ultrasonication time	$X_4$	2	8	min
Dependent variables		Constraints		
Vesicle size	$Y_1$	Medium		nm
Zeta potential	$Y_2$	Maximum		-mV
Polydispersity index	$Y_3$	Minimum		
Entrapment efficiency	$Y_4$	Maximum		%

X-ray diffractometer) using Cu-K $\alpha_1$  (wavelength 1.54 Å) radiation as a source. The samples were scanned in the range of 5–80° in operating voltage 35 kV and current was 40 mA.<sup>[27]</sup>

##### DSC study

The thermal behavior of pure BBN-HCl, soya lecithin, cholesterol, lyophilized unloaded TEs, and BBN-HCl-loaded TEs was determined using a Differential Scanning Calorimeter (DSC 6000, Pyris 6 DSC, PerkinElmer, Waltham, USA). The sample (5 mg) was taken into an aluminum pan in the calorimeter for analysis. Then, the initial condition of sealed pans was kept at 30°C for 10 min. Two-point calibration of instrument was done using indium and zinc. Heating is followed in the temperature range 30–250°C at heating rate 10°C/min under 20 ml/min flow of nitrogen gas.<sup>[28]</sup>

##### TEM study

The shape, size, and surface morphology of TEs were analyzed using TEM. TEM image of optimized BBN-HCl-loaded TEs was observed by TEM (TALOS-200 kV, S-FEG, FEI, USA). A drop of transethosomal suspension was placed on a grid and examined after air drying. TEM grid used of Ted Pella Prod No. 1754-F, Support films, Formvar/Carbon 400 mesh, Cu. To visualize vesicles, negative staining was done using phosphotungstic acid 0.2% (w/v) for 5 min and placed at the accelerating voltage of 200 kV.

##### In vitro release study

Dissolution studies of BBN-HCl loaded TEs were performed using the dialysis bag method as reported (Utreja *et al.*, 2019). The dialysis bag (12 kDa) (surface area = 17.36 ± 1.20) containing 5 ml of transethosomal suspension was placed on dialysis membrane-110 (HiMedia, LA395-20 x 1MT). Dialysis membrane was placed in double-distilled water for 24 h, before experiment starts. The transethosomal loaded membrane placed in phosphate buffer solution (pH 5.5). After, flask containing transethosomal suspension loaded membrane is placed in BOD incubator shaker. The entire arrangement was maintained temperature at 37 ± 0.5°C and speed set to be 60 RPM. At different time intervals, sample collected and amount of BBN-HCl released was measured by UV-Spectroscopy 429 nm. The drug release data were studied in three replicates ( $n = 3$ ) in terms of mean ± S.D.<sup>[29]</sup>

### Stability studies of TEs

The stability study of BBN-HCl-loaded TEs was carried out to study any changes occurs in optimized formulations during storage. As per ICH Q1A (R2) guidelines, the optimized TEs stored at two temperatures, refrigerated temperature ( $4 \pm 1^\circ\text{C}$ ) and room temperature ( $25 \pm 1^\circ\text{C}$ ) in a stability chamber over a period of 6 months. The particle size, ZP and EE of BBN-HCl-loaded TEs were analyzed at different time intervals for 6 months to study stability.<sup>[28]</sup>

### CLSM study of skin

The accumulation in different layers of the skin and permeation of BBN-HCl-loaded TEs was analyzed by CLSM (Olympus, IX83, FV1200MPE, Tokyo, Japan) using rhodamine-B as a dye. The optimized transthesosomal formulation was investigated in the skin of Wistar rat. The formulation was applied to the skin of Wistar rat non-occlusively for a period of 8 h. Then, animal was sacrificed through cervical dislocation and sample skin was removed. The animal tissue was preserved in Carnoy's fluid. Furthermore, 1 mm<sup>2</sup> size of skin samples was obtained by thick tissue cross-sectioning for confocal microscopy study of skin samples. Skin samples were analyzed using 559 nm diode laser as excitation source with objective 0.4 NA. The Olympus Fluoview version 4.2a advance software is was used for depth measurement.<sup>[30]</sup>

### Ex vivo skin permeation study

The permeation and retention studies on the skin were performed using static Franz diffusion cell (area 1.6 cm<sup>2</sup>). The study on Wistar rat skin was approved and obtained permission from the Institutional Animals Ethics Committee approval no. SRIP/IAEC/2019-20/191/09. The Wistar rat's skin epidermis was used as a skin model. It is mounted between the donor and receptor compartment with facing up *stratum corneum* side. Then, lipid eliminated from the skin and washes the tissue part in 0.9% saline. Receptor compartment filled with PBS and donor compartment is filled with BBN-HCl-loaded TEs.

After permeability studies, skin retention study was assessed by amount of drug present in the skin. It is evaluated by taking treated skin samples and homogenized with methanol in homogenizer. Then, it was centrifuged at 7000 rpm for 10 min. Finally, supernatants were filtered through membrane having 0.45 µm size and BBN-HCl was quantified by HPLC.<sup>[31]</sup>

## Statistical Analysis

The statistical analysis was carried out using Design-Expert software (Version 13, trial version, stat ease, MN). All measurements are taken 3 times repeatedly and analysis performed at significant level of  $P < 0.05$ .

## RESULTS AND DISCUSSION

### Box-Behnken Design

Box-Behnken experimental design was most proficient and significant method than other designs for screening of independent variables in minimum runs.<sup>[32]</sup> For the development of BBN-HCl-loaded TEs, the prediction of the main effect of independent variable on dependent variables was important. Four factors were selected as independent variables on the

basis of literature survey and four responses were decided as dependent variables which mostly affected the TEs. The independent variables with their levels are shown in Table 1 and the dependent variables response observation is shown in Table 2. The actual and predicted values of optimized transthesosomes for each response of dependent variables are shown in Table 3.

### Preparation and Optimization of BBN-HCl-loaded TEs

BBN-HCl-loaded TEs were produced using hot homogenization method efficiently. The varying amount of soya lecithin, oleic acid, and ethanol concentration in their composition and different formulations of TEs were produced. The optimized TEs were selected on the basis of their VS, ZP, PDI, and EE. A total of 24 formulations were prepared and optimized through Design-Expert, version 13 software. Among all of the formulations, formulation no. 20 is selected as optimized transthesosomal formulation (OBT-20) on the basis of maximum EE, ZP, minimum PDI, and desired size range of vesicles between 200 and 300 nm which will be best suited for drug permeation and retention in skin layers.

### Effect of Independent Variables on VS ( $Y_1$ )

The VS of TEs varied from 185 to 435 nm [Table 2]. The response surface plot confirms that the independent variables lipid concentration, oleic acid, ethanol concentration, and sonication time possess significant influence on VS [Figure 1]. The quadratic equation which shows correlation between two variables for optimized TEs was given below.

$$Y_1 = 217.6 + 42.13X_1 - 22.26X_2 - 14.56X_3 - 35.86X_4 + 28.28X_1X_2 - 7.17X_1X_3 + 19.13X_1X_4 - 10.22X_2X_3 + 30.92X_2X_4 - 88.08X_3X_4 + 58.95X_1^2 + 27.75X_2^2 - 61.85X_3^2 + 2.34X_4^2 \quad \text{Eq (3)}$$

The positive coefficient value of lipid concentration ( $X_1$ ) in above equation suggested that with the increase in lipid concentration, the VS increases. The negative coefficient value of oleic acid ( $X_2$ ), ethanol concentration ( $X_3$ ), and sonication time ( $X_4$ ) indicates that while increasing in these variables decreased the VS. Due to the higher amount of oleic acid in the formulation size of TEs decreased, it may be due to the bilayer stabilization. The size of course globules was reduced by increasing the sonication time.<sup>[26]</sup>

### Effect of independent variables on ZP ( $Y_2$ )

The ZP of TEs varied from -17.34 to -24.35 mV [Table 2]. The negative ZP values obtained because of soya lecithin and cholesterol presence on the surface of TEs.<sup>[33]</sup> The response surface plot confirms that the independent variables lipid concentration, oleic acid, and sonication time possess significant influence on ZP [Figure 2]. The quadratic equation which shows correlation between two variables for optimized TEs was given below.

$$Y_2 = -18.83 + 1.52X_1 + 0.02X_2 - 0.21X_3 + 0.14X_4 + 0.35X_1X_2 + 0.36X_1X_3 + 1.66X_1X_4 + 1.74X_2X_3 - 0.86X_2X_4 + 0.83X_3X_4 - 1.38X_1^2 - 0.95X_2^2 - 0.58X_3^2 + 0.28X_4^2 \quad \text{Eq (4)}$$

The positive coefficient value of lipid concentration ( $X_1$ ), oleic acid ( $X_2$ ), and sonication time ( $X_4$ ) in above equation suggested that with the increase in these variables, partially



**Table 2:** Observed response of independent variables and dependent variables employed with Box–Behnken design batches

Run	LC (%) $X_1$	OA (mg) $X_2$	EC (%) $X_3$	ST (min) $X_4$	VS (nm) $Y_1$	ZP (–mV) $Y_2$	PDI $Y_3$	EE (%) $Y_4$
1	2	80	30	2	425.2±5.26	–21.91±0.34	0.286±0.048	82.65±1.55
2	2	50	20	2	355.5±6.25	–20.35±0.05	0.325±0.035	78.24±0.82
3	1	50	30	2	295.7±2.86	–23.75±0.80	0.265±0.010	70.15±1.85
4	2	80	20	5	288.5±3.25	–19.10±0.45	0.178±0.256	75.67±1.28
5	3	20	30	5	371.8±6.60	–22.10±0.68	0.270±0.008	80.08±2.05
6	3	80	30	5	435.5±9.28	–24.34±0.81	0.301±0.065	81.98±1.03
7	1	80	30	5	186.8±6.14	–18.79±0.61	0.186±0.021	72.34±1.91
8	2	50	20	8	207.1±2.45	–20.58±0.29	0.281±0.038	80.02±2.12
9	2	80	30	8	190.9±4.11	–19.39±0.50	0.250±0.005	68.25±1.99
10	2	20	30	8	188.9±4.81	–16.23±0.02	0.181±0.049	76.01±0.78
11	3	50	40	5	386.1±2.87	–21.62±0.86	0.253±0.010	79.04±1.78
12	3	50	30	8	378.1±4.52	–17.35±0.37	0.298±0.093	75.46±0.32
13	1	50	40	5	207.5±3.78	–23.10±0.65	0.200±0.005	68.05±1.10
14	1	50	20	5	190.8±3.12	–22.78±0.28	0.280±0.027	71.83±0.82
15	2	80	40	5	378.0±4.13	–18.78±0.46	0.268±0.018	76.98±0.60
16	1	20	30	5	198.7±2.90	–16.34±0.70	0.201±0.078	67.45±0.87
17	2	20	40	5	236.6±3.61	–18.91±0.12	0.162±0.002	72.92±0.13
18	2	20	20	5	262.8±4.84	–21.07±0.06	0.268±0.056	76.08±1.62
19	3	50	20	2	416.6±9.76	–23.01±0.04	0.321±0.091	85.21±1.58
20	2	20	30	5	251.1±7.76	–20.14±0.76	0.141±0.015	84.12±0.65
21	2	50	40	8	202.8±3.87	–18.20±0.23	0.196±0.010	69.67±1.31
22	3	50	30	2	401.7±5.00	–19.35±0.54	0.268±0.009	80.54±0.70
23	1	50	30	8	185.1±2.80	–17.45±0.63	0.189±0.027	67.05±0.82
24	2	50	40	2	368.6±6.98	–22.13±0.98	0.231±0.043	77.17±0.93

VS: Vesicle size, ZP: Zeta potential, PDI: Polydispersity index, EE: Entrapment efficiency

**Table 3:** Actual and predicted values of optimized transethosomes for each response

Serial number	Response	df	F	P-value	Actual value	Predicted value	Residual	R <sup>2</sup>
1	Vesicle size	13	100.92	<0.0001	251.1	260.6	–9.5	0.9826
2	Zeta Potential	13	18.20	<0.0001	–20.14	–21.27	–1.13	0.9067
3	Polydispersity index	13	6.00	0.0038	0.141	0.171	–0.03	0.7345
4	Entrapment efficiency	13	25.71	<0.0001	84.12	80.90	3.22	0.9149

ZP increases. The negative coefficient value of ethanol concentration ( $X_3$ ) indicates insignificant influence on ZP.

#### Effect of independent variables on PDI ( $Y_3$ )

The PDI of TEs varied from 0.141 to 0.321 [Table 2]. The response surface plot confirms that the independent variables lipid concentration, oleic acid, ethanol concentration, and sonication time possess insignificant influence on PDI [Figure 3]. The quadratic equation which shows correlation between two variables for optimized TEs was given below.

$$Y_3 = 0.2065 - 0.012X_1 - 0.0343X_2 - 0.006X_3 - 0.008X_4 - 0.024X_1X_2 + 0.001X_1X_3 - 0.030X_1X_4 + 0.012X_2X_3 + 0.021X_2X_4 - 0.013X_3X_4 + 0.022X_1^2 + 0.013X_2^2 + 0.034X_3^2 + 0.004X_4^2 \quad \text{Eq (5)}$$

The negative coefficient value of lipid concentration ( $X_1$ ), oleic acid ( $X_2$ ), ethanol concentration ( $X_3$ ), and sonication time ( $X_4$ ) suggested all variables possess insignificant influence

on PDI. It indicates that while increasing in these variables decreased the PDI of TEs.

#### Effect of independent variables on EE ( $Y_4$ )

The EE of total 24 TEs varied from 67.05 to 85.21% [Table 2]. The response surface plot confirms that the independent variables lipid concentration, oleic acid, ethanol concentration, and sonication time possess significant influence on EE [Figure 4]. The quadratic equation which shows correlation between two variables for optimized TEs was given below.

$$Y_4 = 72.22 + 3.06X_1 - 2.26X_2 + 1.24X_3 + 2.86X_4 + 5.12X_1X_2 + 2.95X_1X_3 + 1.38X_1X_4 - 0.91X_2X_3 + 4.07X_2X_4 - 4.06X_3X_4 + 4.57X_1^2 + 1.29X_2^2 - 0.61X_3^2 + 1.05X_4^2 \quad \text{Eq (6)}$$

The positive coefficient value of lipid concentration ( $X_1$ ), ethanol concentration ( $X_3$ ), and sonication time ( $X_4$ ) in above equation suggested that with the increase in these variables,

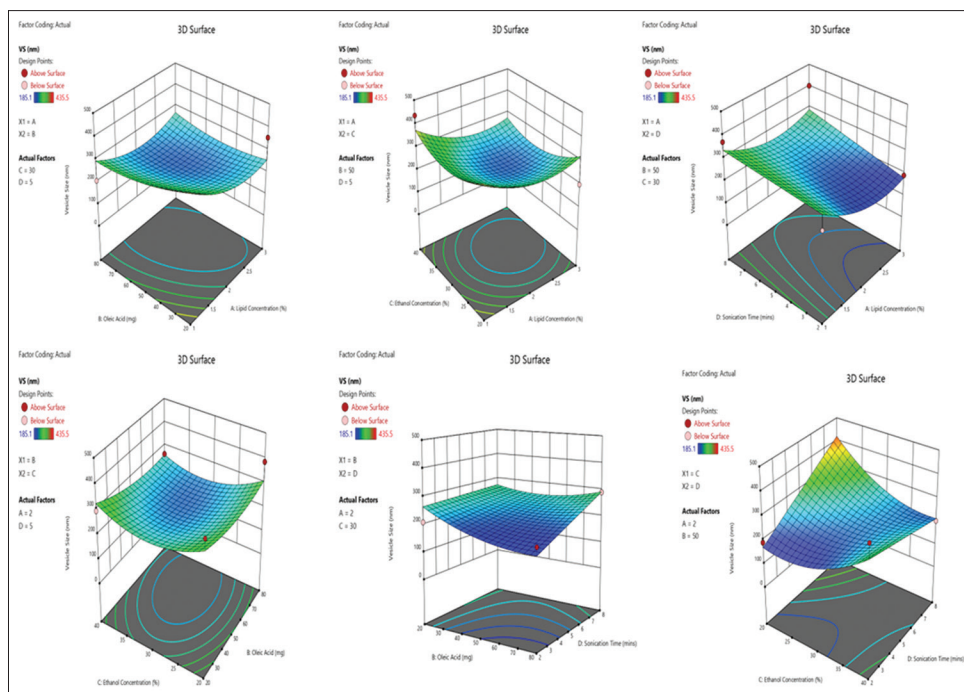


Figure 1: Response surface plot for vesicle size

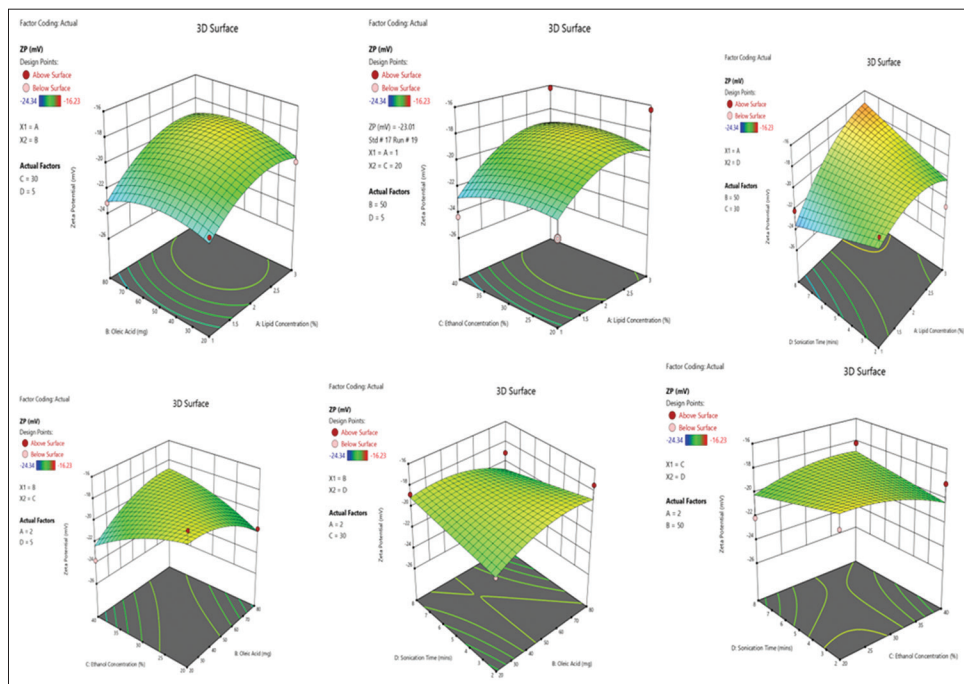


Figure 2: Response surface plot for zeta potential

the EE increases. The negative coefficient value of oleic acid ( $X_2$ ) indicates insignificant influence on EE. Increase in concentration of lipid increases EE in TEs because of higher amount of lipid present for encapsulation.<sup>[34]</sup> While increasing in ethanol concentration, entrapment of drug increases at certain level, further it decreases. In sonication time, entrapment of drug increases with contact time increases, so maximum drug was entrapped in TEs.

## Characterization and Evaluation of Optimized BBN-HCl-Loaded TEs

### VS, ZP, and PDI measurement of BBN-HCl-loaded TEs

For effective transdermal drug delivery system, the VS of TEs plays an important role in penetration, especially into the deeper layers of the skin. The VS, ZP, and PDI of optimized BBN-HCl TEs were found to be 251 nm, -20 mV, and 0.14.

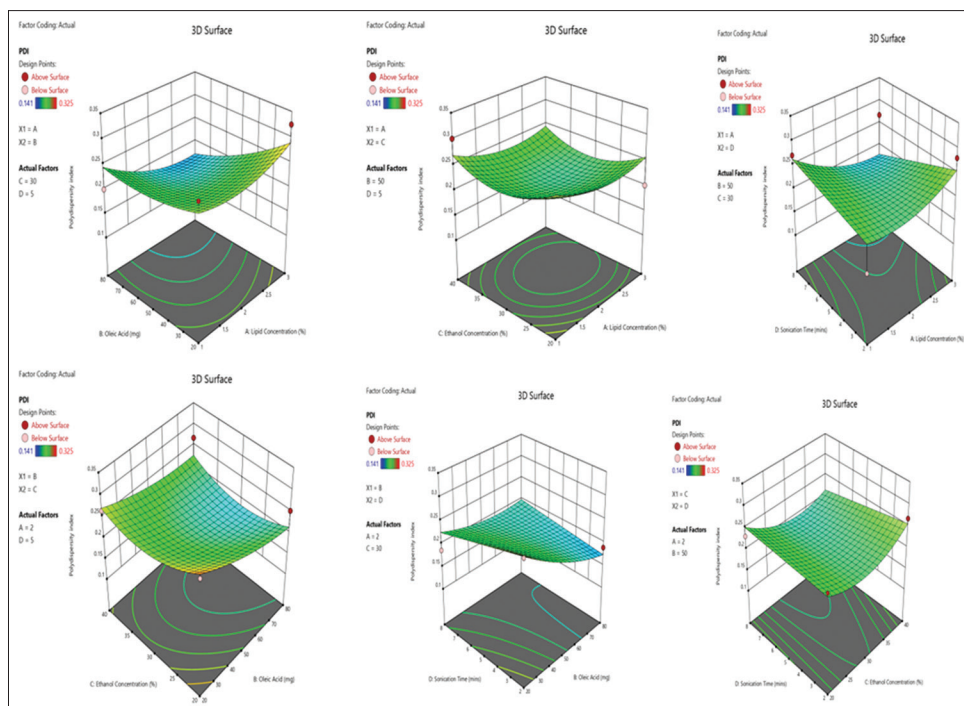


**Figure 3:** Response surface plot for polydispersity index

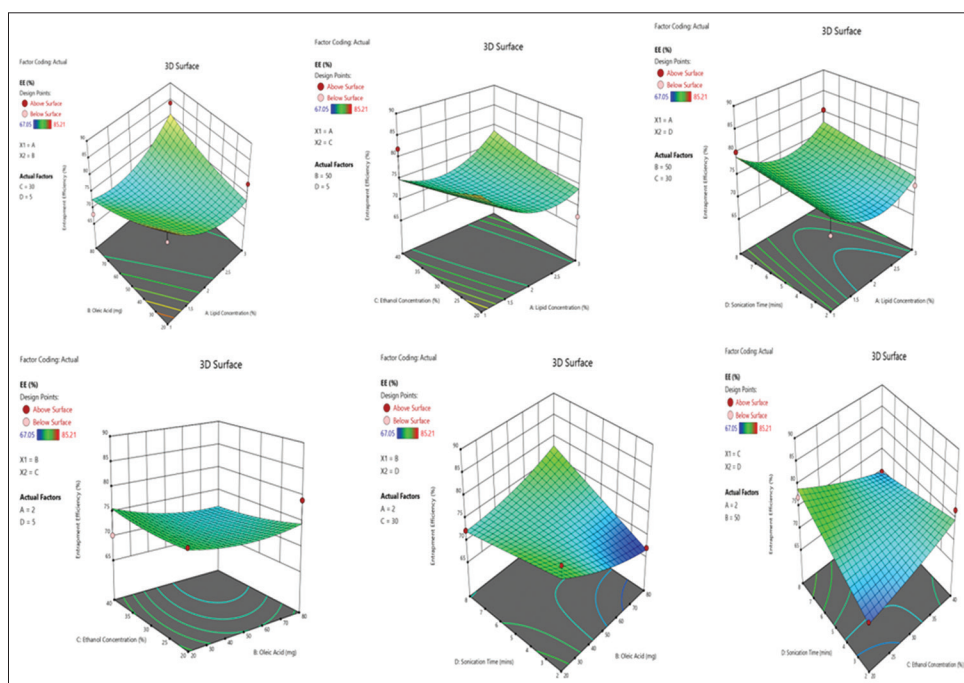


**Figure 4:** Response surface plot for entrapment efficiency

According to literature survey, researchers revealed in their studies, vesicular carriers having size below 400 nm are penetrated efficiently into the deeper layers of skin.<sup>[34]</sup> The mean VS of BBN-HCl-loaded TEs was obtained in the range of 185–435 nm [Table 2]. The VS of optimized TEs is shown in Figure 5. The VS, ZP, PDI, and EE of various TEs are shown in Table 2.

The surface charge or ZP of TEs was also determined by same instrument in the range from +100 mV to –100 mV. The ZP of optimized TEs is shown in Figure 6. Low ZP (up to  $\pm 5$  mV charges) indicates agglomeration and high ZP (more than  $\pm 30$  mV charge) shows excellent monodispersity with good stability. Size distribution of particles observed by PDI usually in the range from 0.1 to 0.5 values. The lesser the value of PDI

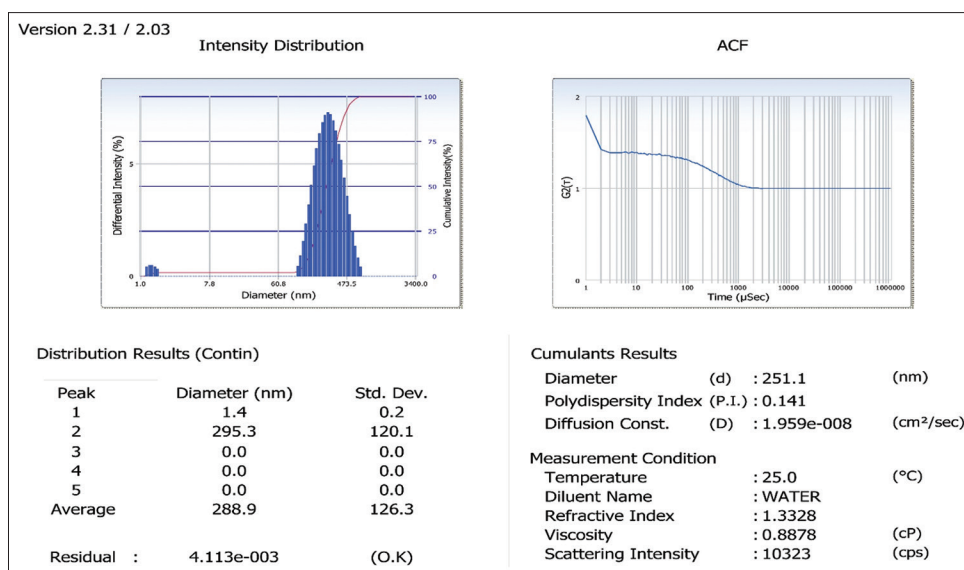


**Figure 5:** Particle size and polydispersity index of optimized TE<sub>s</sub> formulation

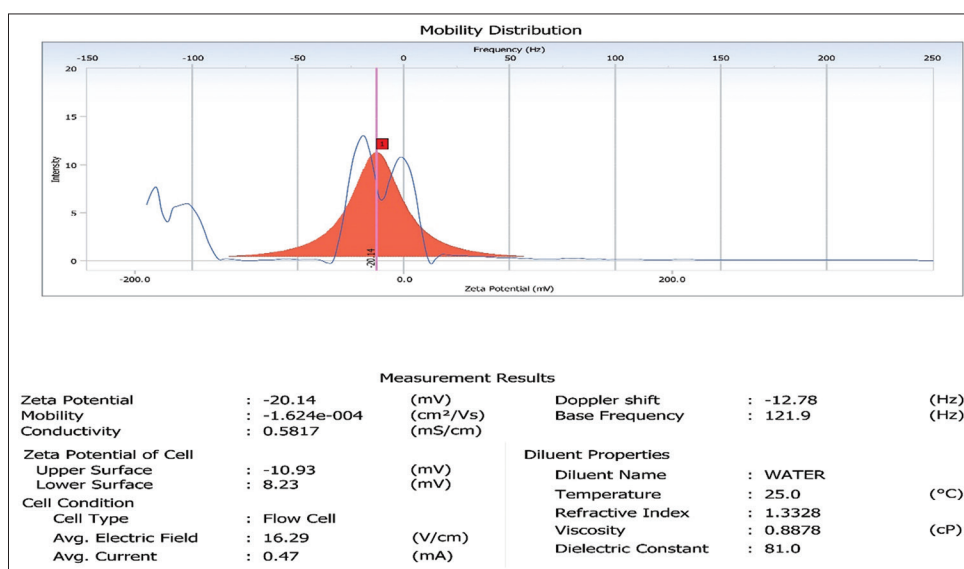


**Figure 6:** Zeta potential of optimized TE<sub>s</sub> formulation

indicates size distribution of particles better homogeneity.<sup>[35]</sup> The PDI is shown in Figure 5.

#### Drug loading capacity and entrapments efficiency

The drug loading and EE of optimized BBN-HCl-loaded TE<sub>s</sub> were found to be 3.62% and 84.2%, respectively. Every lipid has their own loading capacity, after reaching that drug loading cannot increase.<sup>[26]</sup> The size of BBN-HCl-loaded TE<sub>s</sub> increases with increasing the concentration of lipid soya lecithin. Further increase in concentration of lipid, loading capacity decreased and size of TE<sub>s</sub> also decreased, this may be due to the bilayer stabilization. Hence, the formulation indicates that TE<sub>s</sub> are to be explored for transdermal drug delivery due to their good drug loading capacity, high entrapment efficient, and better colloidal stability.

#### P-XRD studies

The powder X-ray patterns of pure BBN-HCl, soya lecithin, cholesterol, and BBN-HCl-loaded TE<sub>s</sub> are depicted in Figure 7. The increase or decrease in crystallinity shown peaks in diffractometer indicates solubility of drug in lipid matrix of TE<sub>s</sub>. The pure BBN-HCl showed major sharp and intense peaks at 2θ values of 6.8, 9.1, and 23.7 in the diffractogram. Cholesterol exhibited peaks at 5.1, 15.4, 16.9, and 32.1 while soya lecithin shows peaks at 19.3 and 19.4. These peaks show that all are crystalline in nature. The peaks of BBN-HCl are disappeared in loaded TE<sub>s</sub> diffractogram. Disappearance of characteristic peaks in diffraction pattern of TE<sub>s</sub> indicates that the BBN-HCl was present in amorphous nanodispersion form. If BBN-HCl is located outside the TE<sub>s</sub> due to its low solubility, crystallization may form and affect the diffraction pattern. These results are concordant with the previous findings by



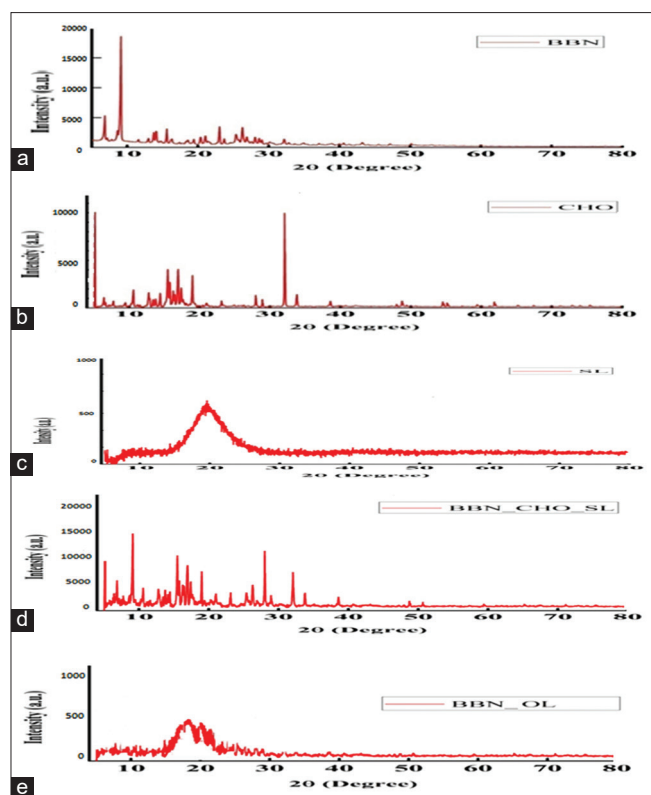


**Figure 7:** XRD graph of (a) BBN-HCl, (b) cholesterol, (c) soya lecithin, (d) physical mixture, and (e) drug-loaded TEs

Sahu *et al.*, 2014, and Utreja *et al.*, 2019. Hence, this indicates that in formulation, BBN-HCl may be successfully encapsulated and it no longer exists in crystalline form in TEs.

#### DSC study

It is a technique in which thermal behavior of any compound was determined by melting point. Thermal behavior of BBN-HCl, soya lecithin, cholesterol, empty TEs, and BBN-HCl-loaded TE is shown in Figure 8. The thermogram of BBN-HCl shows sharp peak at 193°C in the form of endothermic peak. The thermogram of soya lecithin showed sharp endothermic peak at 109°C and a less sharp peak at 176°C while cholesterol showed endothermic peak at 148°C. In empty TEs, endothermic peaks shifted their position slightly of lipids may be due to the decrease in their crystallinity and this observation also supported by XRD analysis. The absence of BBN-HCl endothermic peaks in drug-loaded TE indicates that either effective entrapment BBN-HCl inside TE or soluble in the lipid matrix. Verma *et al.*, 2014, confirmed encapsulation of clotrimazole inside oleic acid vesicles through DSC thermogram study, while Bodade *et al.*, 2013,<sup>[36]</sup> observed similar thermal behavior of ethosomes loaded with repaglinide (RPG) for transdermal delivery. These results suggested that the transethosomal nanocarriers are effectively to be used in transdermal drug delivery system for the treatment of various skin disorders.

#### Transmission electron microscopic (TEM) study

Transmission electron microscope was used to evaluate the shape and surface morphology of BBN-HCl-loaded TE. TEM images are shown in Figure 9 and images reveal that TEs are

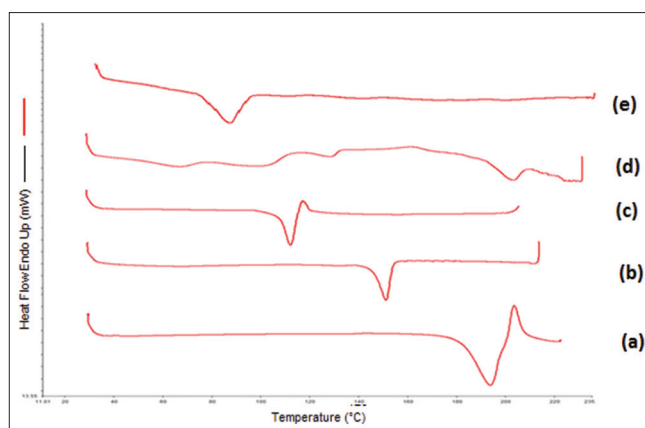


**Figure 8:** DSC thermograms of (a) BBN-HCl, (b) cholesterol, (c) soya lecithin, (d) physical mixture, (e) drug-loaded transethosomes

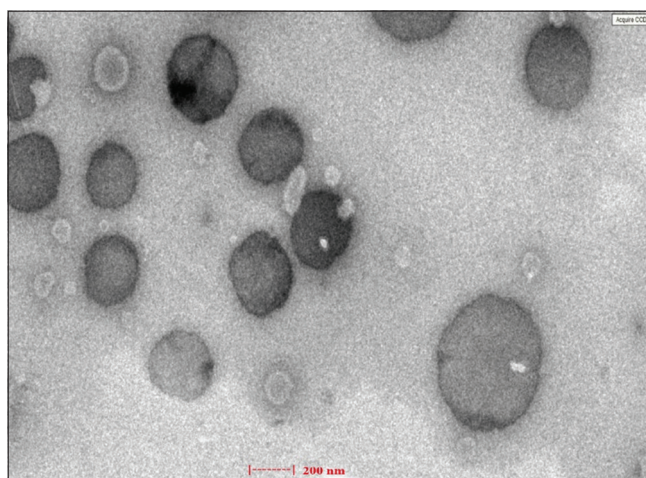


**Figure 9:** TEM image of BBN-HCl-loaded transethosomes

spherical in shape. VS of optimized TE was in between the size range of 250 and 300 nm.

#### In vitro drug release study

Drug release profile of optimized BBN-HCl-loaded TE and pure BBN-HCl solution was studied in phosphate buffer pH 5.5 as dissolution medium for a period of 24 h. The *in vitro* drug release graphs are shown in Figure 10. The release study suggested that factors such as drug-lipid concentration, ethanol concentration, and VS play a major role in increase and decrease the percent of BBN-HCl release from different TE. The optimized BBN-HCl-loaded TE suspension showed  $(81.21 \pm 3.54\%)$  cumulative percentage drug release. The optimized BBN-HCl-loaded TE formulation exhibited a biphasic release pattern. Initially, 40% of the drug released during the 1<sup>st</sup> h followed by slowly sustained release pattern reaching 65% after 12 h. The first burst release is likely due to the small size of the nanoparticles because the small particles provided more surface area to release the drug. In other side, pure BBN-HCl solution released 100% drug within 8 h; however, the release pattern was sustained when it is loaded into TE. This reveals that the TE are potential carriers for prolonged and sustained delivery of BBN-HCl as compared to pure drug solution. After, to determine the release mechanism, results data were fitted in

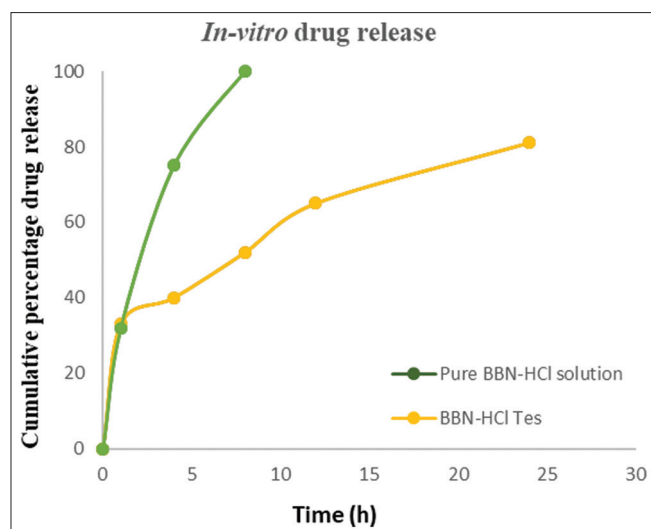


**Figure 10:** *In vitro* drug release studies. Values are expressed as mean  $\pm$  standard deviation ( $n = 3$ )

different models such as Hixson-Crowell and Higuchi matrix. Increase in lipid concentration and ethanol concentration decreased the berberine hydrochloride release from TEs.

#### Stability studies

As per ICH guidelines Q<sub>1</sub>A (R2), the optimized BBN-HCl-loaded TEs were evaluated for size, ZP and EE at various time intervals for 180 days. The optimized BBN-HCl-loaded TEs evaluated at two temperatures, that is, 4°C and 25°C with 75% RH. It was found that the optimized TEs shown negotiable changes after 100 days but some significant variation in their size, ZP and EE after 125 days at both temperatures. After further completion of 180 days, the variation in size was noted about 12% and EE reduced to 9% at room temperature as compared to freezing temperature Figure 11b. It occurs may be due to the leakage and aggregation of TEs which are clearly seemed in TEM images in Figure 11a. However, changes in ZP are about 1% which was negotiable. These results are concordant with the results of the previous study by Utreja *et al.*, 2019. These stability studies suggested that the BBN-HCl-loaded TEs are more stable till 125 days at a temperature of 4°C and 25°C with 75% RH.

#### CLSM studies

The CLSM images revealed enhanced cell internalization and deeper penetration of drug into the different layers of the skin which is clearly shown in Figure 12. The efficacy of optimized TE20 was also investigated by CLSM by utilizing rhodamine-B instead of BBN-HCl. First, skin treated with rhodamine-B containing hydroalcoholic solution which confirmed less distribution of dye in different layers of the skin while the skin treated with fluoro-labeled optimized TE20 showed accumulation and deep penetration of the dye which reaches into the different layers of the skin. These images reveal the effective permeation of TEs vesicles throughout the different layers of the skin. These findings are concordant with the results of earlier research work carried out by Albash *et al.*, in which they showed enhanced transdermal delivery of olmesartan medoxomil through skin<sup>[30]</sup> and Aameeduzzafar

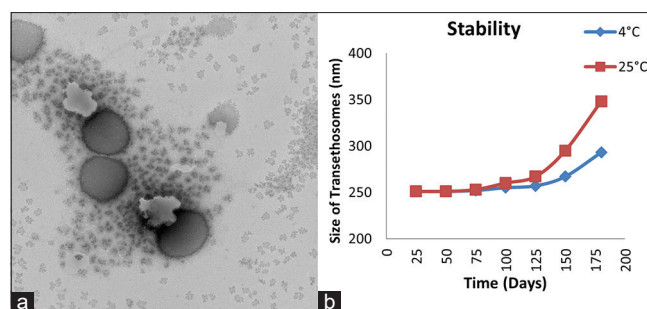


**Figure 11:** (a) Leakage of drug from loaded transethosomes and (b) stability studies of BBN-HCl-loaded transethosomes with respect to VS ( $n = 3$ )

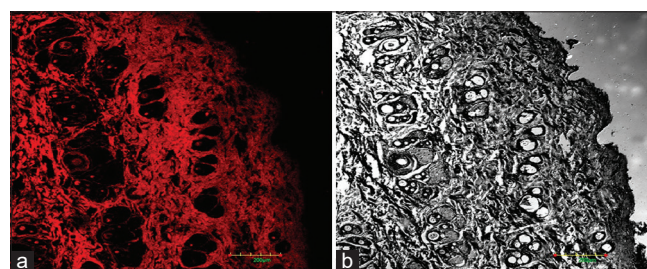


**Figure 12:** Confocal laser scanning microscopy photomicrograph of rat skin treated with rhodamine-B-loaded TEs: (a) Fluorescent light and (b) transmitted light

*et al.* also showed enhanced skin permeation of optimized LAC niosomal gel.<sup>[37]</sup> These findings confirmed accumulation of BBN-HCl in different skin layers and facilitate herbal ethosomal technology used for enhanced transdermal delivery.

#### Ex vivo study

Different type of animal models used instead of human skin to evaluate permeation of drugs. The *ex vivo* permeation study was performed using rat skin model. The formulation 20 was optimized that BBN-HCl TEs (OBT-20) are shown in Table 2. The study indicated that the amount of BBN-HCl permeated from optimized TEs (OBT-20) was higher as compared to BBN-HCl solution.  $J_{\max}$  of BBN-HCl TEs and BBN-HCl solution was found to be  $86.26 \pm 6.63 \mu\text{g}/\text{cm}^2/\text{h}$  and  $12 \pm 1.15 \mu\text{g}/\text{cm}^2/\text{h}$ . The lower permeability is due to the lower log *P*-value of BBN-HCl. The greater permeation of BBN-HCl TEs over drug solution indicates good elasticity of oleic acid vesicles and presence of ethanol facilitates additional penetration of the vesicles into the skin layers.<sup>[38]</sup> Furthermore, around 63.16% of BBN-HCl permeated across the skin at the 4<sup>th</sup> h which was significantly higher than BBN-HCl solution, which was only 16% at the same point.

## CONCLUSION

BBN-HCl-loaded TEs were successfully developed by modified hot method. The Box-Behnken design approach was used to optimize and screen the independent variables with most effective dependent variables for the development of transethosomal formulations. In this study, two formulation factors concentration of lipid, concentration of ethanol, and one process factor sonication time were found most significant factors on response variables. The optimized BBN-HCl-loaded

TEs showed high stability with high EE, obtained desired VS, and prolonged release of drug. Topical penetration of TEs in deeper skin layers confirmed the assessment of enhanced cell internalization. Based on the results of this research work, it can be considered as the optimized BBN-HCl-loaded TEs could be a promising and potential carrier for effective transdermal drug delivery system to enhance the delivery of BBN-HCl drug into deeper layers of the skin and minimizes the disadvantages of topical marketed formulations to overcome stratum corneum barrier problem, antifungal resistance, high-dose frequency, toxicity, and low permeation of drug to the targeted site.

## ACKNOWLEDGMENTS

The authors are grateful to Indian Herbs Extractions Ltd. (U.K, India) for providing pure BBN-HCl as a gift sample. The authors acknowledge FIST supported TEM facility to the Department of Chemistry, IISER, Bhopal, for providing TEM facility. The authors are thankful to CIF, IISER, Bhopal, for providing DLS, DSC, and XRD facility. The authors are also grateful to SIC-A National Facility, IIT, Indore, for providing CLSM study. The authors are also thankful to the Management and Principal of Shri Rawatpura Sarkar Institute of Pharmacy, Kumhari, for providing research laboratory and necessary infrastructural facilities for this work.

## FUNDING

None.

## CONFLICTS OF INTEREST

The work is originally done in our laboratory. The authors report no conflicts of interest, financial, or otherwise.

## REFERENCES

- Almandil NB. Healthcare professionals awareness and knowledge of adverse drug reactions and pharmacovigilance. *Saudi Med J* 2016;37:1359-64.
- Tanner T, Marks R. Delivering drugs by the transdermal route: Review and comment. *Skin Res Technol* 2008;14:249-60.
- Mishra KK, Kaur CD, Verma S. Transthesosomes and nanoethosomes: Recent approach on transdermal drug delivery system. In: Farrukh MA, editor. *Nanomedicines*. IntechOpen: E-Publishing Inc.; 2019. p. 33-50.
- Chen J, Lu WL, Gu W, Lu SS, Chen ZP, Cai BC. Skin permeation behavior of elastic liposomes: Role of formulation ingredients. *Expert Opin Drug Deliv* 2013;10:845-56.
- Song CK, Balakrishnan P, Shim CK, Chung SJ, Chong S, Kim DD. A novel vesicular carrier, transthesosome, for enhanced skin delivery of voriconazole: Characterization and *in vitro/in vivo* evaluation. *Colloids Surf B Biointerfaces* 2012;92:299-304.
- Imanshahidi M, Hosseinzadeh H. Pharmacological and therapeutic effects of *Berberis vulgaris* and its active constituent, berberine. *Phytother Res* 2008;22:999-1012.
- Zhu L, Zhang D, Zhu H, Zhu J, Weng S, Dong L, *et al.* Berberine treatment increases Akkermansia in the gut and improves high-fat diet-induced atherosclerosis in Apoe<sup>-/-</sup> mice. *Atherosclerosis* 2018;268:117-26.
- Zhang SL, Chang JJ, Damu GL, Fang B, Zhou XD, Geng RX, *et al.* Novel berberine triazoles: Synthesis, antimicrobial evaluation and competitive interactions with metal ions to human serum albumin. *Bioorg Med Chem Lett* 2013;23:1008-12.
- Choudhary VP, Sabir M, Bhide VN. Berberine in giardiasis. *Indian Pediatrics* 1972;9:143-6.
- Swabb EA, Tai YH, Jordan L. Reversal of cholera toxin-induced secretion in rat ileum by luminal berberine. *Am J Physiol* 1981;241:G248-52.
- Lin TH, Kuo HC, Chou FP, Lu FJ. Berberine enhances inhibition of glioma tumor cell migration and invasiveness mediated by arsenic trioxide. *BMC Cancer* 2008;8:58.
- Sun Y, Xun K, Wang Y, Chen X. A systematic review of the anticancer properties of berberine, a natural product from Chinese herbs. *Anticancer Drugs* 2009;20:757-69.
- Pang B, Zhao LH, Zhou Q, Zhao TY, Wang H, Gu CJ, *et al.* Application of berberine on treating type 2 diabetes mellitus. *Int J Endocrinol* 2015;2015:905749.
- Kong W, Wei J, Abidi P, Lin M, Inaba S, Li C, *et al.* Berberine is a novel cholesterol-lowering drug working through a unique mechanism distinct from statins. *Nat Med* 2004;10:1344-51.
- Fatehi-Hassanabad Z, Jafarzadeh M, Tarhini A, Fatehi M. The antihypertensive and vasodilator effects of aqueous extract from *Berberis vulgaris* fruit on hypertensive rats. *Phytother Res* 2005;19:222-5.
- Mishra KK, Kaur CD, Sahu AK, Panik R, Kashyap P, Mishra SP. Medicinal plants having antifungal properties. In: *Medicinal Plants - Use in Prevention and Treatment of Diseases*. Raipur, India: Intechopen: E-Publishing Inc.; 2020. p. 1-14.
- Peng L, Kang S, Yin Z, Jia R, Song X, Li L, *et al.* Antibacterial activity and mechanism of berberine against *Streptococcus agalactiae*. *Int J Clin Exp Pathol* 2015;8:5217-23.
- Sahibzada MU, Sadiq A, Faidah HS, Khurram M, Amin MU, Haseeb A, *et al.* Berberine nanoparticles with enhanced *in vitro* bioavailability: Characterization and antimicrobial activity. *Drug Des Devel Ther* 2018;12:303-12.
- Awate PS, Pimple TP, Pananchery JF, Jans AS. Formulation and evaluation of berberine hcl as niosomal drug delivery system. *Asian J Pharm Res* 2020;10:149-59.
- Zhu JX, Tang D, Feng L, Zheng ZG, Wang RS, Wu AG, *et al.* Development of self emulsifying drug delivery system for oral bioavailability enhancement of Berberine HCl. *Drug Dev Ind Pharm* 2013;39:499-506.
- International Conference on Harmonization of Technical Requirement for Registration of Pharmaceuticals for Human Use, ICH Harmonizes Tripartite Guideline, "Quality Risk Management", Q9 Step 4; 2005.
- Jones R. Pharmaceutical manufacturing: How to understand the process and assess the risks to patient safety. *Pharm Eng* 2009;29:1-10.
- Gupta B, Poudel BK, Pathak S, Tak JW, Lee HH, Jeong JH, *et al.* Effects of formulation variables on the particle size and drug encapsulation of imatinib-loaded solid lipid nanoparticles. *AAPS PharmSciTech* 2016;17:652-62.
- Shrivastava S, Gidwani B, Kaur CD. Development of mebendazole loaded nanostructured lipid carriers for lymphatic targeting: Optimization, characterization, *in-vitro* and *in-vivo* evaluation. *Particulate Sci Technol* 2021;39:380-90.
- Elsheikh MA, Elnaggar YS, Hamdy DA, Abdullah OY. Novel cremochylomicrons for improved oral bioavailability of the antineoplastic phytochemistry berberine chloride: Optimization and pharmacokinetics. *Int J Pharm* 2018;535:316-24.
- Sahu A, Jain V. Screening of process variables using Plackett-Bruman design in the fabrication of gedunin-loaded liposomes. *Artif Cells Nanomed Biotechnol* 2016;44:1-12.
- Kumar S, Narayan R, Ahammed V, Nayak Y, Nayak UY. Development of ritonavir solid lipid nanoformulations by Box Behnken design for intestinal lymphatic targeting. *J Drug Deliv Sci Technol* 2017;44:181-90.
- Utreja P, Kumar L. Formulation and characterization of transthesosomes for enhanced transdermal delivery of propranolol

- hydrochloride. *Micro Nanosyst* 2019;11:1-10.
29. Verma S, Bhardwaj A, Vij M, Bajpai P, Goutam N, Kumar L. Oleic acid vesicles: A new approach for topical delivery of antifungal agent. *Artif Cells Nanomed Biotechnol* 2014;42:95-101.
30. Albash R, Abdelbary AA, Refai H, El-Nabarawi MA. Use of transethosomes for enhancing the transdermal delivery of olmesartan medoxomil: *In vitro*, *ex vivo*, and *in vivo* evaluation. *Int J Nanomedicine* 2019;14:1953-68.
31. Ameenuzzafar, Ali J, Bhatnagar A, Kumar N, Ali A. Chitosan nanoparticles amplify the ocular hypotensive effect of catechol in rabbits. *Int J Biol Macromol* 2014;65:479-91.
32. Ameenuzzafar, Qumber M, Alruwaili NK, Bukhari SN, Alharbi KS, Imam SS, *et al.* BBD-based development of itraconazole loaded nanostructured lipid carrier for topical delivery: *In-vitro* evaluation and antimicrobial assessment. *J Pharm Innov* 2021;16:85-98.
33. Szcześ A. Effects of DPPC/cholesterol liposomes on the properties of freshly precipitated calcium carbonate. *Colloids Surf B Biointerfaces* 2013;101:44-8.
34. Das S, Ng WK, Kanaujia P, Kim S, Tan RB. Formulation design, preparation and physicochemical characterizations of solid lipid nanoparticles containing a hydrophobic drug: Effects of process variables. *Colloids Surf B Biointerfaces* 2011;88:483-9.
35. Al-Kassas R, Wen J, Cheng AE, Kim AM, Liu SSM, Yu J. Transdermal delivery of propranolol hydrochloride through chitosan nanoparticles dispersed in mucoadhesive gel. *Carbohydr Polym* 2016;153:176-86.
36. Bodade SS, Shaikh KS, Kamble MS, Chaudhari PD. A study on ethosomes as mode for transdermal delivery of an antidiabetic drug. *Drug Deliv* 2013;20:40-6.
37. Qumber M, Ameenuzzafar, Imam SS, Ali J, Ahmad J, Ali A. Formulation and optimization of lacidipine loaded niosomal gel for transdermal delivery: *In-vitro* characterization and *in-vivo* activity. *Biomed Pharmacother* 2017;93:255-66.
38. Zafar A. Development of oral lipid based nano-formulation of dapagliflozin: Optimization, *in vitro* characterization and *ex vivo* intestinal permeation study. *J Oleo Sci* 2020;69:1389-401.